Survival of Fossilised Diatoms and Forams in Hypervelocity Impacts with Peak Shock Pressures in the 1 – 19 GPa Range

Burchell M.J.[1*], Harriss K.H.[1], Price M.C.[1], Yolland L.[1,2]

[1] Centre for Astrophysics and Planetary Science, School of Physical Sciences, Univ. of Kent, Canterbury, Kent CT2 7NH, United Kingdom.

[2] Now at: Computational Life and Medical Sciences Network, University College London, 20 Gordon Street, London WC1H, United Kingdom.

***Contact author: Mark J Burchell**
Contact address: Centre for Astrophysics and Planetary Science, School of Physical Sciences, Univ. of Kent, Canterbury, Kent CT2 7NH, United Kingdom.
Contact email: M.J.Burchell@kent.ac.uk
Contact Phone: +44 1227 827833

Abstract:

Previously it has been shown that diatom fossils embedded in ice could survive impacts at speeds of up to 5 km s^{-1} and peak shock pressures up to 12 GPa. Here we confirm these results using a different technique, with diatoms carried in liquid water suspensions at impact speeds of 2 to 6 km s^{-1}. These correspond to peak shock pressures of 3.8 to 19.8 GPa. We also report on the results of similar experiments using forams, at impact speeds of 4.67 km s^{-1} (when carried in water) and 4.73 km s^{-1} (when carried in ice), corresponding to peak shock pressures of 11.6 and 13.1 GPa respectively. In all cases we again find survival of recognisable fragments, with mean fragment size of order 20 – 25 µm. We compare our results to the peak shock pressures that ejecta from giant impacts on the Earth would experience if it subsequently impacted the Moon. We find that 98% of impacts of terrestrial ejecta on the Moon would have experienced peak pressures less than 20 GPa if the ejecta were a soft rock (sandstone). This falls to 82% of meteorites if the ejecta were a hard rock (granite). This assumes impacts on a solid lunar surface. If we approximate the surface as a loose regolith, over 99% of the impacts involve peak shock pressures below 20 GPa. Either way, the results show that a significant fraction of terrestrial meteorites impacting the Moon will do so with peak shock pressures which in our experiments permit the survival of recognisable fossil fragments.

Key words: Astrobiology, Moon, Impact Processes

Highlights:

- Laboratory studies of hypervelocity impacts show that fossil fragments can survive shock pressures of up to 20 GPa
- These shock pressures are similar to those terrestrial impact ejecta are subject to when impacting the Moon
- The surviving fragments are typically of 20 to 25 µm

This paper has been accepted for publication in Icarus, March 2nd 2017

1. Introduction

It is now well established that planets are not isolated bodies, and that impact ejecta arising from giant impacts on even planet-sized bodies can produce ejecta which escapes the struck body and enters interplanetary space. This explains, for example, lunar (e.g. Marvin, 1983) and Martian meteorites (e.g. Bogard and Johnson, 1983) here on Earth. Terrestrial material can also be ejected by the same mechanism, and indeed once in interplanetary space can even exit the solar system via a close encounter with Jupiter (although it is unlikely to then enter another stellar system, see Melosh 2003). A special case for terrestrial ejecta, is where the material is intercepted by the Moon (Armstrong *et al*., 2002). As pointed out for example by Armstrong (2010), such impacts on the Moon are typically at what, in Solar System terms, is a relatively low impact speed of just a few km s^{-1} (with a peak at around 3 km s^{-1}), so material should readily survive such impacts. How such terrestrial material might then be preserved on the Moon is discussed for example by Crawford *et al*. (2008).

In parallel to this insight concerning the successful transfer of material from body to body, has been the re-emergence of the idea called panspermia (Arrhenius 1908, or see Burchell 2004 for a review), with the view that life forms may also similarly transfer between bodies. After all, if the material of which planets are made can be successfully ejected into space, why should it not carry life? This "rocky road to panspermia" (Melosh 1988), or litho-panspermia, opened up the possibility that the long disputed theory of panspermia might indeed have a sound footing. One issue however, was that whilst during ejection the rocky material would only be lightly shocked and life might survive ejection (proposed by Melosh, 1988, demonstrated in the laboratory for example by Burchell *et al*., 2003 and Fajardo-Cavazos *et al*., 2009), sterilisation can occur during the transfer in interplanetary space. This is due to the ambient radiation. Further, during the impact on a new body there would be a greater, again possibly sterilising, shock. The hazards during transfer have been discussed by, amongst others, Mileikowski *et al*. (2000), Clark *et al*. (1999), and Clark (2001). Whilst radiation would have sterilised all currently identified Martian meteorites on Earth (due to the combination of their small size and their long occupancy times in interplanetary space), it was pointed out that, for example, the minimum Mars-Earth transfer time in an unpowered orbit is about 7 months, so radiation effects were not a priori an obstacle to successful transfer of life. This left shock as the potentially crucial element permitting/disallowing viable transfer of life.

In the 1990s, it was often assumed that extreme shocks were sterilising events. However, Burchell *et al*. (2000), pointed out that this was not actually proven experimentally. They suggested that even if survival rates were less than 1%, this was still of interest as even 1 cc of terrestrial soil could typically contain 10^8 microorganisms, spores etc. To test the possibility of survival in the shocks of extreme impacts, Burchell et al. (2000), reported firing microorganism-rich projectiles at a variety of targets at speeds of 3.8 to 4.9 km s^{-1}. They reported one successful experiment, but noted that confirmation was needed, and, in a later paper, Burchell *et al*. (2001), confirmed the result (equivalent to shocks at around 70 – 80 GPa). Separately, Horneck *et al*. (2001), supplied an extreme shock (order 32 GPa) to a sample via explosive shock loading and they also found survival of viable material. In these

examples, survival was at a low rate (10^{-4} to 10^{-6}) and decreased with increasing pressure (e.g. Burchell *et al*., 2004 and 2007, Stöffler *et al*., 2007, Horneck *et al*., 2008, and Price *et al*., 2013). By contrast, similar experiments have shown that seeds are less hardy, and suffer extensive damage even in shocks around 1 GPa (Jerling *et al*. 2008, Leighs *et al*., 2012).

However, there is a parallel question to the survival of life in shock events, namely the survival of fossils. Even if life on a planet like Mars had developed and then died, it could leave traces as fossils. Therefore rocks ejected between planets might be considered more likely to carry fossils rather than active state or spore state lifeforms. This idea jumps into prominence from time to time, e.g. the putative fossils claimed in ALH84001 (McKay *et al*., 1996). It also underpins the idea of searching for the Earth's fossil record by looking for terrestrial meteorites (astropalaeontology) on the Moon (Armstrong *et al*., 2002; Gutiérrez 2002, Armstrong 2010). Thus, to find evidence for life elsewhere, we no longer have to worry about life itself surviving transit hazards such as radiation, long transit times etc. Nevertheless, implicit in such discussions is that the fossils will survive shock events in a recognizable form.

Recently, the survival of fossils in extreme shocks has been demonstrated by Burchell *et al*. (2014). They used diatom fossils embedded in ice and fired these in a two stage light gas gun into targets of water. The water was then filtered and diatom fossil material extracted. They did this work at impact speeds of 0.388 to 5.34 km s^{-1} (equivalent to shock pressures of 0.2 to 19 GPa). The impact speed range is similar to that for impacts of terrestrial meteorites on the Moon, but given the dissimilar materials involved it is not clear if the shock pressure range is equivalent or not.

Here we revisit this topic. We again fire diatom fossils in a two stage light gas gun, but do so via a different technique, suspending the fossils in liquid water in the sabot rather than in ice. Varying the technique shows the general validity of the results so far. We then expand the work further to include shock survival of examples of fossilised foraminifera (forams for short) in similar experiments. The forams are made of calcium carbonate, as compared to the silica of the diatoms skeletons. This allows us to see if the results depend on the nature of the materials used as well as the magnitude of the shock pressure. We also calculate the pressure range for terrestrial meteorites impacting the Moon and compare to those achieved in the experiments to date.

2. Method

We used commercially available diatomaceous earth as a source of diatom skeletons. As well as intact and fragmented diatom skeletons (see Fig. 1), it also contained silicoflagellate skeletons such as that of Dictyocha speculum - a type of microfossil known since the early Cretaceous. For the forams we used *Nummulite variolarius*, which originated from the London Clay bed. Example images of the forams before shooting are shown in Fig. 2. The forams used were typically of order 1 mm in diameter. This was larger than the diatoms which were or order 100 to 200 μm pre-shot. Given the (relatively) large size of the forams, only 9 were loaded in each shot.

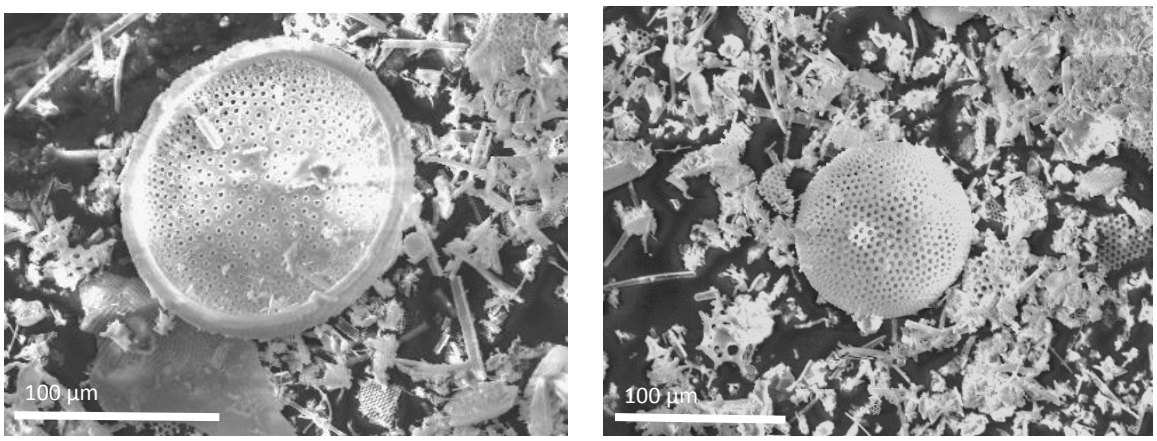

Fig. 1. Examples of diatom skeletons pre-shot (each example shows a single large intact diatom on a background of smaller fragments).

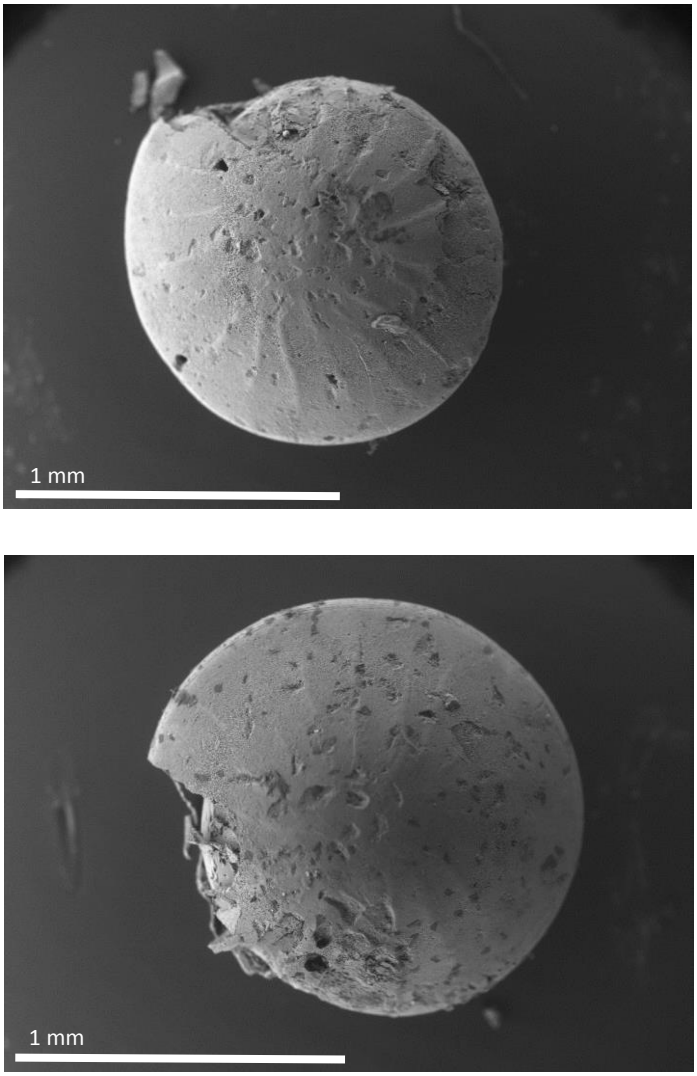

Fig. 2. Examples of intact foram skeletons pre-shot.

The material to be shot was suspended in water and loaded into nylon sabots (nylon density 1184 kg m^{-3}). In this work, two types of sabots were used, those which carried ice and those which carried liquid water. The ice bearing sabots were similar to those in Burchell et al. (2014). The sabots were cylinders, 4.3 mm in length and 4.5 mm in diameter. They had a central shaft drilled into them along the main axis, this shaft was 3 mm in length and 3 mm in diameter. Material to be shot was placed in the shaft, water added to fill the cavity, and then the sabot was frozen to -20 ºC. The water bearing sabots were also formed from a single piece of nylon machined into cylinders with a hollow central well along part of their length (see Fig. 3). The sabot external diameter was again 4.5 mm and it was 4.3 mm long. The diameter of the hollow shaft however was only 2.5 mm and it was also 2.5 mm deep. The top 0.5 mm of the shaft was counter sunk below the surface of the sabot. The central well was loaded when the sabots were stood vertical such that a small meniscus of water stood proud of the sabot. An acetate lid (0.25 mm thickness and 3 mm dia.) was then slid across the top of the sabot into the counter bored top of the well and sealed in place with Loctite superglue. This method was used to ensure there was no cavity behind the lid and that the central well in the sabot was completely filled (avoiding cavitation effects during shock loading).

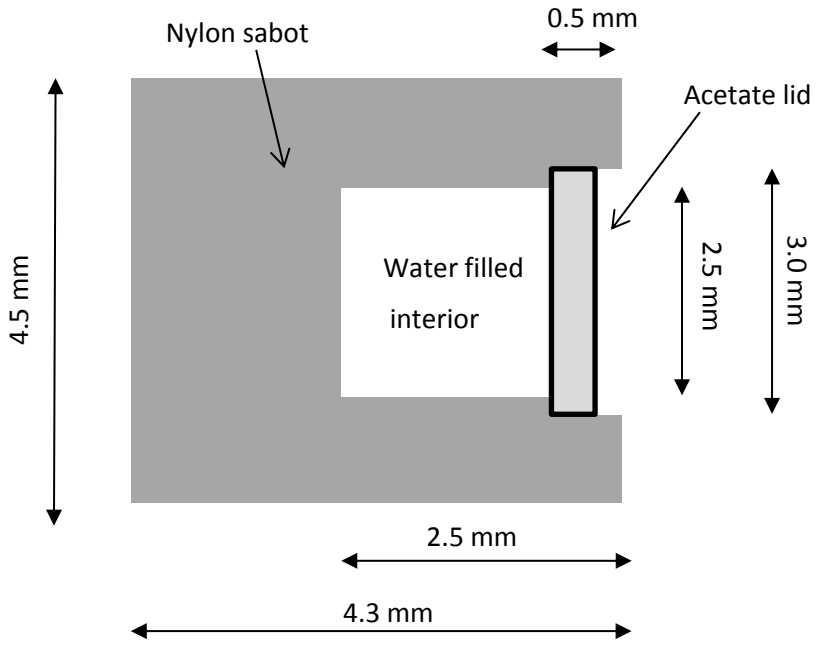

Fig. 3. Schematic cross section of a nylon sabot as used in this work. The acetate lid was 0.25 mm thick. The sabot as shown would be fired horizontally moving toward the right.

Once loaded, the sabot was mounted in a two stage light gas gun and fired. The gun that was used at the University of Kent can have its shot speed adjusted in each shot by varying the

amount of gun powder, pre-shot pressure in the launch tube etc. (see Burchell *et al*., 1999). The speed was measured in each shot to within ±1%. In the present work, 5 shots were carried out, with speeds of 2.17, 4.67, 4.72, 4.73 and 6.12 km s^{-1} (see Table 1). Three of the shots (at 2.17, 4.72 and 6.12 km s^{-1}) used diatoms, and two (at 4.67 and 4.73 km s^{-1}) used forams. The diatom shots were all made using used water bearing sabots, in order to contrast the results with earlier work which fired diatoms in ice. The shots also extended the speed range to over 6 km s^{-1}. The two foram shots had one carried in ice, and one with water, in the sabot, permitting a comparison with the diatom data.

Table 1: Shot parameters and peak shock pressure (calculated for water impacting water using the PIA as described in the text).

Impact speed (km s^{-1})	**Peak Shock Pressure (GPa)**	**Projectile Material**
2.17	4.2	Diatoms in water
4.67	11.6	Forams in ice
4.72	13.0	Diatoms in water
4.73	13.1	Forams in water
6.12	19.8	Diatoms in water

The targets used were bags of water held in a box whose entrance was a small hole in the line of flight of the sabot, and which stood in a tray. During impact the water target was disrupted, but the scattered water was caught and drained into the tray. The target chamber was maintained at 50 mbar pressure during the shots.

After each shot the target assembly was removed from the gun and the water filtered through Whatman filter paper. The collected material was then placed on a SEM stub and examined in a Hitachi S3400N scanning electron microscope.

3. Experimental Results

Using the SEM, the filtered debris from each shot was repeatedly scanned and several measurements made. We first looked at the diatom shots. Intact specimens were relatively frequent at the lower speeds, but rare at the highest speeds although we did find examples (see Fig. 4). We then looked at the fragments in each diatom shot (see Fig. 5 for examples). In each shot we measured the size of a number of fragments (to provide a mean size), plus in addition we recorded the size of both the largest and second largest fragments we could locate in the shot. The idea of measuring the largest fragment was to look for the maximum survival size in a shot. The reason for also measuring the second largest was in case we had either incomplete recovery from the target or incomplete discovery in the SEM images. The results are given in Table 2. The uncertainly given on the mean in Table 2 is the standard error on the mean, the size distributions themselves are broader.

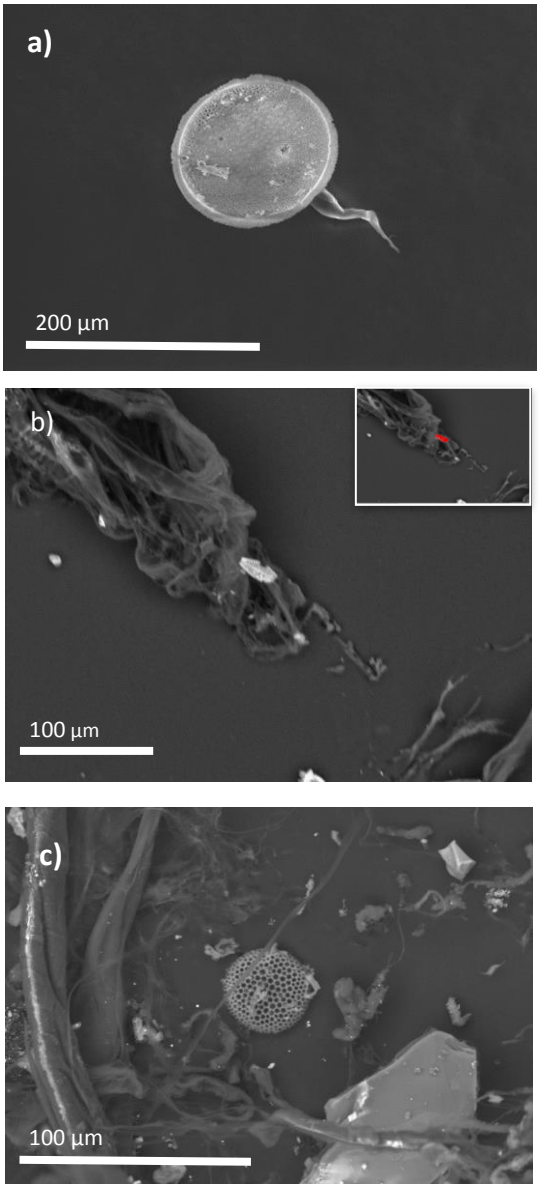

Fig. 4. Example recovered intact diatoms. (a) 2.17 km s^{-1}, (b) 4.72 km s^{-1} and (c) 6.12 km s^{-1}.

Table 2: Size of recovered fossil fragments in each shot.

Impact Speed (km s^{-1})	**Fossil type**	**Mean Size (µm)**	**Number of samples**	**Largest fragment size (µm)**	**2nd Largest fragment size (µm)**
0	Diatom	28.8 ± 0.8	500	180	136
0	Foram	1300±30	5	1370	1320
2.17	Diatom	39.0 ± 4.6	32	123	110
4.67	Foram	20.8 ± 1.5	51	73.3	43.4
4.72	Diatom	16.4 ± 4.7	12	44.1	40.8
4.73	Foram	24.9 ± 3.3	56	90.8	72.2
6.12	Diatom	19.0 ± 2.9	14	47.5	45

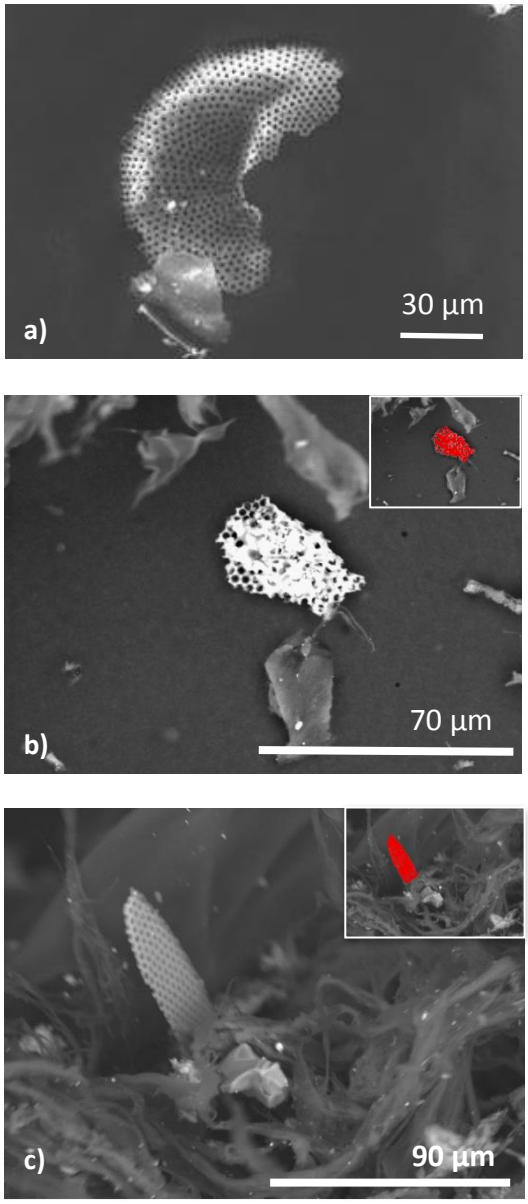

Fig. 5. Example recovered diatom fragments. (a) 2.17 km s^{-1}, (b) 4.72 km s^{-1} and (c) 6.12 km s^{-1}.

We then looked for examples of silicoflagellate skeletons in the diatom shots. We readily found intact examples at all the impact speeds (Fig. 6). This is in contrast with the relative lack of intact diatom fossils. However, we note that different size scales: intact diatoms were of order 100 µm pre-shot, whereas the silicoflagellate skeletons were of order 40 µm. In our previous work we showed that the mean size of diatom fragments after impact was in the range 20 – 30 µm (depending on impact speed), which given the width of these size distributions encompasses many silicoflagellate skeletons in our samples. It is thus not a surprise that these therefore survive with reasonable frequency in our samples after impact.

We next looked at the foram shots. There were no intact forams found after impact. Instead we found fragments in both shots (Fig. 7). The sizes of the fragments are given in Table 2. With mean fragment size of 20 – 25 µm, there was no significant difference in fragment size

between the two foram shots, even though one used liquid water as the carrying medium and the other used ice. Furthermore, the mean fragment size was similar to that observed in the diatom shots, even though the materials (silica and calcium carbonate) are very different and were of different initial size.

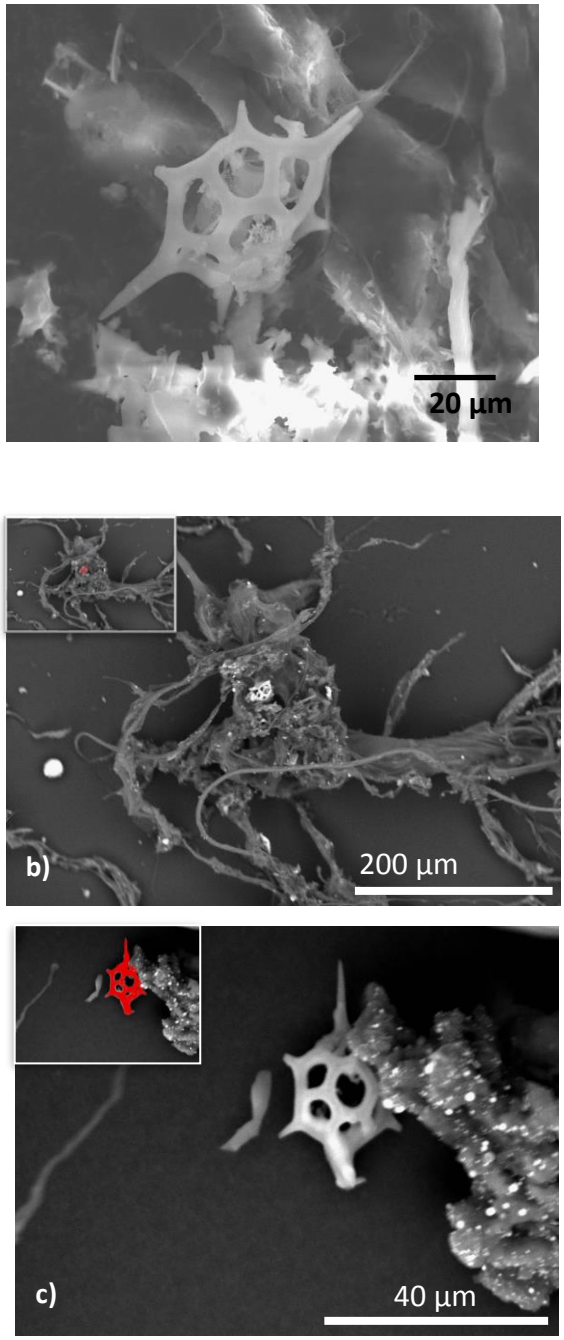

Fig. 6. Examples of recovered silicoflagellate skeletons (which appear intact at all speeds). (a) 2.17 km s^{-1}, (b) 4.72 km s^{-1} and (c) 6.12 km s^{-1}.

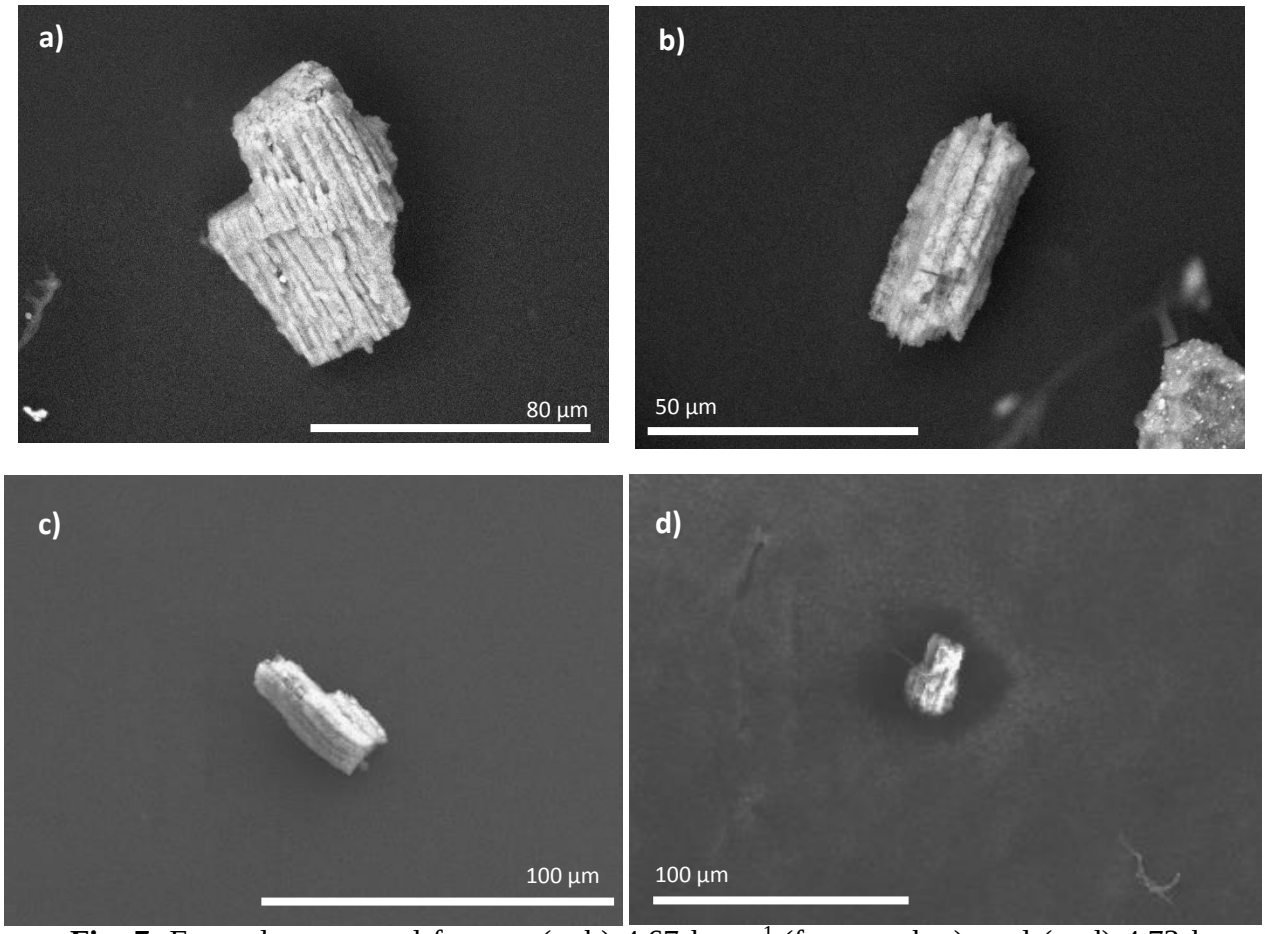

Fig. 7. Example recovered forams. (a, b) 4.67 km s^{-1} (frozen sabot), and (c, d) 4.73 km s^{-1} (liquid water filled sabot).

4. Shock Pressures

4.1 Planar Impact Approximation

To find the shock pressure experienced in each shot we used two approaches. The first was to apply the Planar Impact Approximation (PIA, see Melosh, 2013 for a discussion of the technique). This relies on a linear wave speed equation of the form U = c + Su, where c and S are material dependent coefficients, and are required for both target and projectile. Here we simplify our experimental set-up and assume that either a water or ice projectile has directly impacted a water target. For ice we used c = 1.317 km s^{-1}, S = 1.526, and an ice density of 915 kg m^{-3}, whilst for water we used c = 2.393 km s^{-1}, S = 1.333, and a water density of 997.9 kg m^{-3} (see Melosh, 2013). The results of the PIA at the impact speeds used here are given in Table 1 and cover 4.2 to 19.8 GPa.

4.2 Autodyn Hydrocode

It is also possible to obtain shock pressures using a hydrocode. This involves a more detailed simulation which can include the various materials in the sabot. It provides shock information across the whole of the sample (and not just the most highly shocked region near the impact plane as in the PIA) as well as providing a time history. Here we used the Autodyn hydrocode

(see Hayhurst and Clegg, 1997 for a discussion of this code). The sabot structure was modelled in the simulations, using a 2-D half-space model (with axial symmetry) with 40 Lagrangian cells across the length of the projectile. Autodyn library models were used for water (Bakken and Anderson, 1967) and nylon (Matuska, 1984) with the sample in the sabot consisting of water. It should be noted that no allowance was made for the presence of the fossil material itself, which is assumed to be subject to the shock pressures generated in the water during the impacts. Additionally, as no material model could be found for cellulose acetate, the lid of the sabot was modelled as nylon. Considering the thinness of the lid, and the speed of the projectile, this was deemed a reasonable approximation. Simulations of the sabot carrying an ice sample are contained in Burchell et al. (2014).

Table 3: Shock pressures in the water sample in the projectile as estimated with the Autodyn hydrocode. At each impact speed the maximum and minimum pressures are given, along with the median value (defined as the value exceeded by 50% of the sample).

v (km s^{-1})	Max. Peak pressure (GPa)	Min peak pressure (GPa)	Approx. Median peak pressure (GPa)
2.2	5.6	4.4	4.9
4.7	17.6	13.9	16.9
6.1	27.4	21.1	25.5

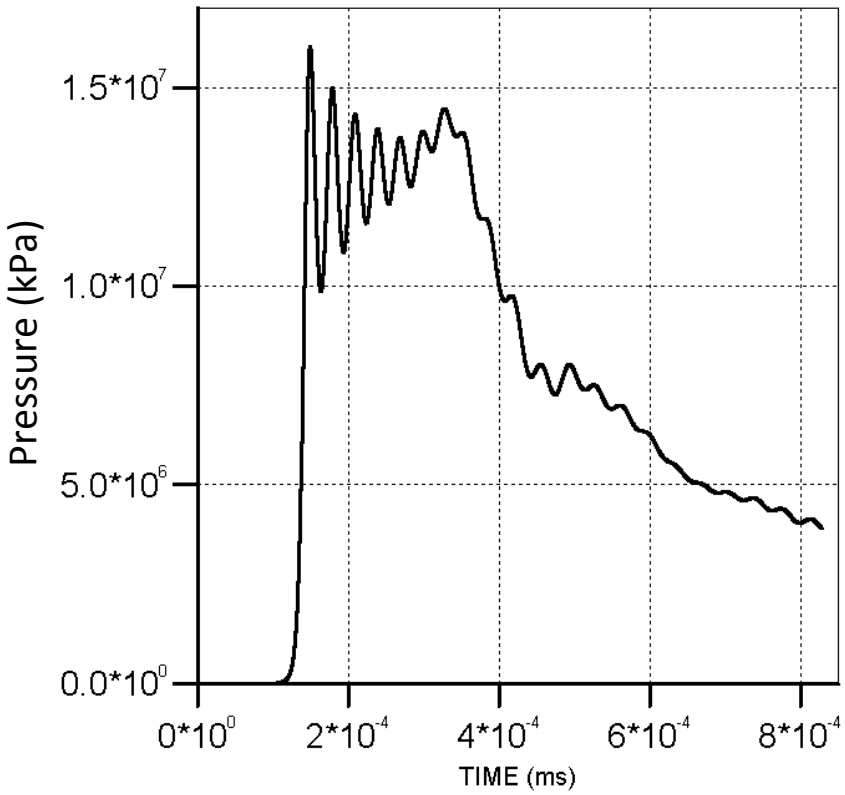

Fig. 8. Time history of peak shock pressure in front region of water in the sabot in an impact at 4.7 km s^{-1}, as simulated in the Autodyn hydrocode.

Three simulations were carried out, at speeds of 2.2, 4.7 and 6.1 km s^{-1} (see Table 3). At each speed three estimates of the peak shock pressure are provided: the peak value anywhere in the water in the projectile, the minimum such pressure, and the median shock pressure defined as that value which was exceeded in 50% of the water. This allows a picture of the pressure across the sample to be obtained. This is important as it is not known in which part of the sample any individual fossil fragment observed after the impact was located. In all three examples in Table 3, the maximum pressures obtained are about $1/3^{rd}$ greater than those indicated by the PIA. The duration of the shock can also be obtained from the hydrocode simulations. In Fig. 8, the pressure vs. time can be seen near the front of the sabot for the simulation at 4.7 km s^{-1}. The peak pressure is maintained for some 0.2 μs, it then falls off but there is an elevated pressure for order of 1 μs.

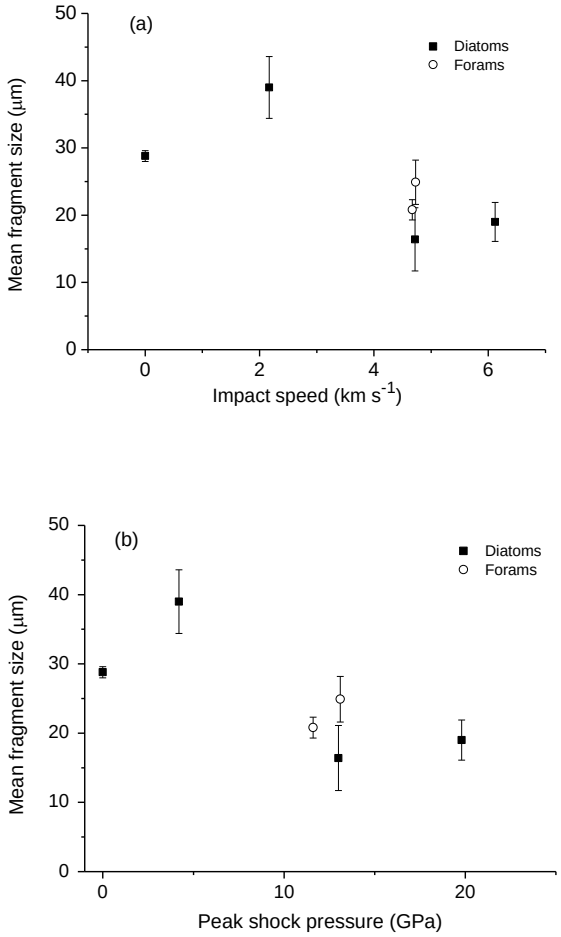

Fig. 9. Mean fragment size vs. (a) impact speed and (b) peak impact shock pressure. The peak pressures were found using the PIA (see main text).

We show the mean fragment size after impact vs. impact speed and peak shot pressure in Fig. 9. The pre-shot data is dominated by already broken fragments in the diatom samples. As soon as impacts occur, the larger diatoms break, giving more large fragments which initially increases the mean fragment size. However by 4+ km s^{-1} (around 10+ GPa), the largest objects observed are below 100 μm and so not only are most diatoms now broken into

smaller fragments, but also any original larger fragments are further reduced in size. This reduces the mean fragment size to around 20 µm. As already noted, the foram and diatom fragments are similar in size at ~4 km s^{-1}, indicating that the different original size and composition do not significantly influence the outcome of the impacts.

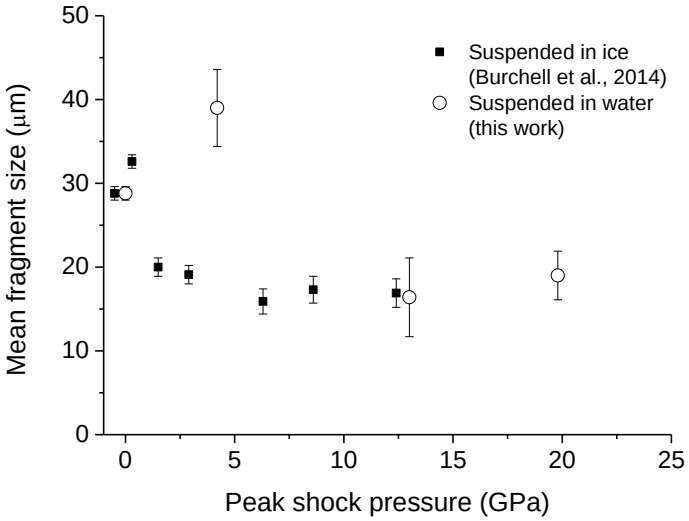

Fig. 10. Comparison of the results here for mean fragment size after impact for diatoms carried in water, with those of Burchell *et al*., 2014 for diatoms fired frozen in ice. Note that the two data points at 0 GPa are the raw samples in each data set, and have been slightly off-set from each other on the x-axis for clarity.

Comparing the diatom results here (from shots where the diatoms were loaded in water in the sabot), to those of Burchell et al. (2014) (where the sabot was frozen) shows little different in the results (Fig. 10) at high shock pressures. In the original (ice) shots at 4 to 5 km s^{-1} (9 – 12 GPa) the mean fragment size was 16 to 17 µm, compared to 19 µm here in that speed range and similar peak shock pressure. We note however that at 4 GPa the new data sits well above the mean fragment size from the earlier work.

5. Discussion

The shock pressures experienced in the impacts of terrestrial meteorites on the Moon were calculated using the PIA. The impact speed distribution for such impacts was calculated by Armstrong 2002. We then used the PIA in two scenarios (with c and S values from Melosh, 2013). First we assumed the ejected terrestrial material was a typical "hard" rock - granite (a typical crustal material) with c = 3.68 km s^{-1}, S = 1.24, and density 2630 kg m^{-3}. It is of course unlikely that fossils would be in a granite (unless the melt cooled after flowing over fragments of sedimentary rock). But it does illustrate the general case of hard rock terrestrial ejecta impacting the Moon. Of more relevance to rocks containing fossils, we also considered Coconino sandstone as the ejected material. This is the type of sandstone the Barringer impact crater (Arizona) formed in. For Coconino sandstone we used c = 1.50 km s^{-1}, S =

1.43, and density 2000 kg m^{-3} (Melosh, 2013). In both cases we assumed a lunar surface made of basalt with c = 2.60 km s^{-1}, S = 1.62, and density 2860 kg m^{-3} (Melosh, 2013).

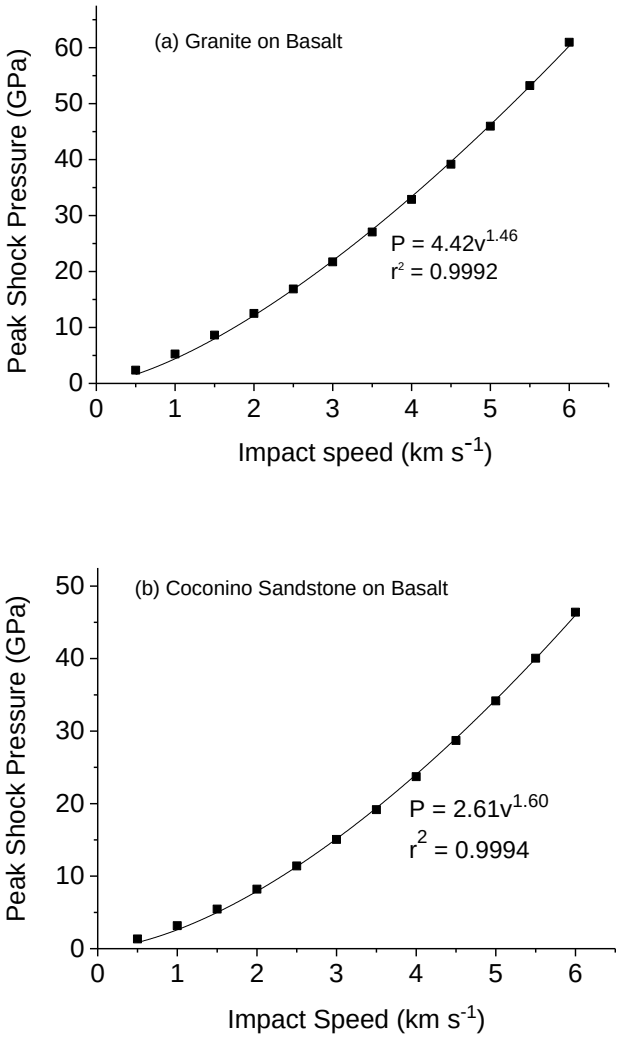

Fig. 11. Impact shock pressures predicted from the PIA (as described in the text) for (a) granite impacting basalt, (b) sandstone impacting basalt. In both cases the shock pressure was calculated at discrete speeds and is indicated by the square symbol. A power law fit (P is shock pressure in GPa and v is the impact speed in km s^{-1}) was then made to the data and is shown by the solid line.

The predicted shock pressure range for impacts on the Moon is shown in Fig. 11 vs. impact speed for both scenarios; case (a) is a granite impactor, b) Coconino sandstone. For impacts of terrestrial ejecta on the Moon, Armstrong (2010) calculated both the absolute magnitude of the impact speed and its vertical component. It is the vertical component which drives the calculation of shock pressures. In Table 6 of Armstrong (2010), it is estimated that 43% of impactors have a vertical component of their speed less than 1 km s^{-1}, 60% have less than 2 km s^{-1}, and 71% less than 2.5 km s^{-1}. Based on Fig. 6 in Armstrong (2010), we estimate that 99% of the impacts have a vertical speed less than 4 km s^{-1}. Armstrong *et al*. (2002), approximated the peak shock pressures in the lunar impacts using the simple formula:

$$P = \frac{2}{3}\,\rho\, v_{vert}^2 \qquad \text{Eqn. 1}$$

In Table 4 we give a range of the vertical component of impact speeds from 1 – 4 km s^{-1}, along with the peak pressure calculated from Eqn. 1 as well as those from the PIA in each scenario used here. It can be seen that whilst eqn. 1 provides a reasonable order of magnitude approximation of peak pressures, it only agrees with the more detailed PIA estimate for sandstone at low pressures (diverging as pressures increase above 10 – 15 GPa), whilst the opposite is true for the harder rock (granite).

Table 4: Peak shock pressures as a function of the vertical impact speed for impacts of granite and sandstone on basalt and sand. Basalt represents impacts on a solid lunar surface, whereas sand represents impacts on a non-consolidated regolith. The probabilities are from Table 6 or Fig. 6 in Armstrong (2010), and represent the fraction of impacts of terrestrial ejecta on the Moon with less than that vertical impact speed. The peak pressures labelled "Eqn. 1" were calculated using Eqn. 1 in the main text (as per Armstrong *et al*., 2002), whilst those labelled "PIA" used linear wave speed relations as given in the main text.

Vertical speed (km s^{-1})	Probability	Peak Pressure (GPa)				
		Eqn. 1	PIA Granite on Basalt	PIA Granite on Sand	PIA Sandstone on Basalt	PIA Sandstone On Sand
1	0.43	2	5.3	3.2	3.2	2.2
2	0.60	8	12.5	7.7	8.2	5.5
2.5	0.71	12	16.9	10.5	11.4	7.5
2.75	0.82	14	19.4	11.9	13.2	8.7
3	0.92	17	21.7	13.5	15.1	9.9
3.5	0.98	23	27.1	16.8	19.2	12.5
4	0.99	31	32.9	20.4	23.7	15.4

We compare the peak shock pressures for lunar impacts (Table 4), with those involved in the experiments presented here (Table 1). We can see that for impacts on solid basalt by an impactor comprised of a rock like sandstone, the peak shock pressures in our fossil experiments (20 GPa) cover 98% of the shock range for impacts of terrestrial ejecta on the Moon. Even for a hard rock (here approximated by granite) impacting solid basalt, 82% of lunar impacts involve shocks with a maximum of 20 GPa.

It was pointed out by Crawford et al. (2008) that since the lunar surface is a regolith, then for smaller impactor size scales (i.e. metre scale), it may be more appropriate to treat the lunar surface as a non-consolidated material (rather than as solid basalt). Crawford et al. (2008) suggested the used of sand as a suitable analogue. To simulate sand in the PIA we used c = 2.10 km s^{-1}, S = 1.113, and density 1610 kg m^{-3} (the high pressure phase coefficients given by Ahrens and Johnson, 1995). As noted by Crawford et al. (2008) the sand has a similar bulk density to the lunar regolith (given as 1660 kg m^{-3} by Carrier et al., 1991). The result (see Table 4) is to lower the peak impact shock pressure found using the PIA for impacts by both

granite (typical 34% reduction) and sandstone (mean reduction of 33%) on sand compared to similar impacts on basalt. In such a scenario, for both types of impactor 99% of impacts generate peak shock pressures lower than those experience by the fossil samples in our experiments.

The impact scenario featured here is a very specific one that leads to relatively low impact speeds and consequent shock pressures. In separate work considering asteroidal and cometary impacts on the Moon, Svetsov and Shuvalov (2015) show that even for impact speeds above 6 km s^{-1}, substantial amounts of projectile material can be expected to be retained in lunar impact craters, albeit with higher shock pressures.

6. Conclusions

Our results show that we can find recognisable fragments of several types of fossilised organisms after impacts at speeds which generate peak impact shock pressures compatible with those for terrestrial impact eject hitting the Moon. In our experiments there appears to be a size effect which is independent of the materials involved. This limits the mean size of the surviving material to around 40 μm at 4.7 km s^{-1} and 20 μm at 6 km s^{-1}, although the range of sizes stretches up to around 20 μm higher than these values, permitting intact survival of silicoflagellates. In the case of silicoflagellates, this is of particular interest as these skeletons have a 3D structure which is preserved. In all cases, very fine detail is also preserved in the recovered materials. When compared to previous work, the use of a liquid suspension for the diatoms (as distinct from previously where they were frozen in ice) does not seem to have had a significant effect on the results.

Whilst these results do not show that terrestrial fossil remains are present in the lunar regolith, it does strongly suggest that they should be present if they can survive the time period since their emplacement. In this respect, the work by, for example Crawford et al. (2008), on how to find preserved terrestrial meteorites on the Moon is particularly relevant.

Acknowledgements

We thank STFC for funding impact studies at the University of Kent. We wish to thank L. Rothschild for suggesting the use of forams in this work.

References

Ahrens, T.J and Johnson, M.L. (1995) Shock wave data for rocks. In *AGU Reference Shelf 3: Rock Physics and Phase Relations, A Handbook of Physical Constants*, edited by T.J. Ahrens, American Geophysical Union, Washington, DC, pp 35–44.

Armstrong J.C. (2010) Distribution of Impact Locations and Velocities of Earth Meteorites on the Moon. Earth Moon Planets **107**, 43 – 54.

Armstrong J.C., Wells L.E., Gonzales G. (2002) Rummaging through Earth's attic for remains of ancient life. Icarus **160**, 183–196.

Arrhenius S. (1908) Worlds in the Making (trans. H. Born). Harper, London.

Bakken L. H. and Anderson P. D. 1967. The complete equation of state handbook. SANDIA SCL-TM-67-118

Bogard D.D., and Johnson P. (1983) Martian Gases in an Antarctic Meteorite? Science **221**, 651 – 654.

Burchell M.J. (2004) Panspermia Today. Int. J. Astrobiology **3**, 73 – 80.

Burchell M.J., Cole M.J., McDonnell J.A.M., Zarnecki J.C. (1999) Hypervelocity Impact Studies Using the 2 MV Van de Graaff Dust Accelerator and Two Stage Light Gas Gun of the University of Kent at Canterbury. Meas. Sci. Tech. **10**, 41-50.

Burchell M.J., Shrine N.R.G, Bunch A.W., Zarnecki J.C. (2000). Experimental Tests of the Impact related Aspects of Panspermia, in *Impacts on the Early Earth* pp. 1-26, eds. I. Gilmour & C. Koeberl, pub. Springer 2000.

Burchell M.J., Mann J., Brunch A.W., Brandão P.F.B. (2001) Survivability of Bacteria in Hypervelocity Impact. Icarus **154**, 545-547.

Burchell M.J., Galloway J.A., Bunch A.W., Brandao P. (2003) Survivability of Bacteria Ejected from Icy Surfaces after Hypervelocity Impact. Origin of Life and Evolution of the Biosphere **33**, 53 – 74.

Burchell M.J., Mann J.R., Bunch A.W. (2004) Survival of Bacteria and Spores Under Extreme Pressures. Monthly Notices of the Royal Astronomical Society **352**, 1273 – 1278.

Burchell M.J. (2007) Survival of microbial life under shock compression: implications for Panspermia. Proceedings of SPIE symposium 6694, identifier 669416, (10 pages).

Burchell M.J., McDermott K.H., Price M.C. (2014) Survival of Fossils Under Extreme Shocks Induced by Hypervelocity Impacts. *Phil. Trans. Roy. Soc*. A, **372**: 20130190.

Carrier W., Olhoeft G.R., Mandell W. (1991) Physical properties of the lunar surface. In *The Lunar Sourcebook*, edited by G.H. Heiken, D.T. Vaniman, and B.M. French, Cambridge University Press, Cambridge, pp 475–594.

Clark B.C. (2001) Planetary interchange of bioactive material: Probability factors and implications. Origins of Life and Evolution of the Biosphere **31**, 185 - 197.

Clark B.C., Baker, A.L., Cheng A.F., Clemett S.J., McKay D., McSween H.Y., Pieters C.M., Thomas P., Zolensky M. (1999) Survival of life on asteroids, comets and other small bodies. Origins of Life and Evolution of the Biosphere **29**, 521 - 545.

Crawford I.A., Baldwin E.C., Taylor E.A., Bailey J.A., Tsembelis K. (2008) On the survivability and detectability of terrestrial meteorites on the Moon. Astrobiology **8**, 242 – 252.

Fajardo-Cavazos P., Langenhorst F., Melosh H.J., and Nicholson W.L. (2009) Bacterial Spores in Granite Survive Hypervelocity Launch by Spallation: Implications for Lithopanspermia. Astrobiology 9, 647 – 657.

Gutiérrez, J.L., (2002) Terrene meteorites in the Moon: Its relevance for the study of the origin of life in the Earth. In Proceedings of the First European Workshop on Exo-Astrobiology, European Space Agency Special Publication, edited by H. Lacoste, ESA SP-518, Noordwijk, Netherlands, pp187-191.

Hayhurst C.J., Clegg R.A. (1997) Cylindrically symmetric SPH simulations of hypervelocity impacts on thin plates. *Int. J. Impact Eng.* **20**, 337–348.

Horneck G., Stöffler D., Eschweiler U., Hornemann U. (2001) Bacterial spores survive simulated meteorite impact. Icarus 149, 285 – 290.

Horneck G., Stöffler D., Ott S., Hornemann U., Cockell C.S., Moeller R., Meyer C., de Vera J.P., Fritz J., Schade S., Artemieva N.A. **(**2008). Microbial rock inhabitants survive hypervelocity impacts on Mars-like host planets: First phase of Lithopanspermia experimentally tested. Astrobiology **8**, 17–44.

Jerling A., Burchell M.J., Tepfer D. (2008) Survival of Seeds in Hypervelocity Impacts. Int. J. Astrobiology **7**, 217 – 222.

Leighs J.A., Hazell P.J., Appleby-Thomas G.J. (2012) The effect of shock loading on the survival of plant seeds. Icarus **220**, 23–28.

Marvin U.B. (1983) The discovery and initial characterization of Allan Hills 81005: The first lunar meteorite. Geophys. Res Letts. 10, 775 – 778.

Matuska D. A. 1984. HULL Users Manual. AFATL-TR-84-59

McKay D.S., Gibson E.K., Thomas Keprta K.L., Vali H., Romanek C.S., Clemett S.J., Chillier X.D.F., Maechling C.R., Zare R.N. (1996) Search for past life on Mars: possible relic biogenic activity in Martian meteorite ALH84001. Science 273, 924–930.

Melosh H.J. (1988) A Rocky Road to Panspermia. Nature **332**, 687 – 688.

Melosh H.J. (2003) Exchange of Meteorites (and Life?) between Stellar Systems. Astrobiolgy **3**, 207 – 215.

Melosh, H. J. (2013) Contact and Compression Stage of Impact Cratering, pp. 32 – 42, in Impact Cratering Processes and Products, Osinski and Pierazzo (eds.), pub. Wiley-Blackwell. ISBN 978-1-4051-9829-5.

Mileikowsky, C., Cucinotta F.A., Wilson J.W., Gladman B., Horneck G., Lindegren L., Melosh J., Rickman H., Valtonen M., and Zheng J.Q. (2000). Natural transfer of viable microbes in space. *Icarus* **145**, 391–427.

Price M.C., Solscheid C., Burchell M.J., Josse L., Adamek N., Cole M.J. (2013) Survival of yeast spores in hypervelocity impact events upto velocities of 7.4 km s^{-1}. Icarus **222**, 263-272.

Stöffler D., Horneck G., Ott S., Hornemann U., Cockell C.S., Moeller R., Meyer C., de Vera J.P., Fritz J., Artemieva N.A. (2007). Experimental evidence for the potential impact ejection of viable micro-organisms from Mars and Mars-like planets. Icarus **186**, 585–588.

Svetsov V.V., Shuvalov V.V. (2015) Water delivery to the Moon by asteroidal and cometary impacts. Planetary and Space Science **117**, 444 – 452.